Available online at www.sciencedirect.com
ScienceDirect
Control Engineering Practice 15 (2007) 197–208
CONTROL ENGINEERING PRACTICE
www.elsevier.com/locate/conengprac

Robust controller design by linear programming with application to a double-axis positioning system

Alireza Karimi*, Marc Kunze, Roland Longchamp

Laboratoire d'Automatique-STI, Ecole Polytechnique Fédérale de Lausanne (EPFL), Station 9, 1015 Lausanne, Switzerland

Received 13 October 2005; accepted 12 June 2006
Available online 7 September 2006

Abstract

A linear programming approach is proposed to tune fixed-order linearly parameterized controllers for stable LTI plants. The method is based on the shaping of the open-loop transfer function in the Nyquist diagram. A lower bound on the crossover frequency and a new linear stability margin which guarantees lower bounds for the classical robustness margins are defined. Two optimization problems are proposed and solved by linear programming. In the first one the robustness margin is maximized for a given lower bound on the crossover frequency, whereas in the second one the closed-loop performance in terms of the load disturbance rejection is optimized with constraints on the new stability margin. The method can directly consider multi-model as well as frequency-domain uncertainties. An application to a high-precision double-axis positioning system illustrates the effectiveness of the proposed approach.

Keywords: Linear programming; Convex optimization; PID controller; Robustness margin

1. Introduction

Many controller design methods are based on optimization techniques. In early works, the main interest was to find an analytical solution to the optimization problem. Recently, with new progress in numerical methods to solve convex optimization problems, new approaches for controller design with convex objectives and constraints have been developed. These methods usually lead to controllers of at least the same order as the plant model. However, design of restricted-order controllers (like PID controller) leads to non-convex optimization problems in the controller parameter space.

Nowadays, PID controllers are still extensively used in industrial applications and a lot of methods have been proposed in the literature to simply tune the controller parameters. H_∞ optimization of fixed-order controllers have been the subject of many research works (Malan et al., 1994; Grigoriadis & Skelton, 1996) which adopt nonlinear and non-convex algorithms. These methods require generally heavy computations and do not guarantee the global optimum to be achieved. Moreover, it is generally difficult to tune the weighting filters automatically. Industrial users prefer classical specifications like gain and phase margins, crossover frequency, maximum of the sensitivity and complementary sensitivity functions and good set point and disturbance rejection responses. A combination of time and frequency-domain specifications makes the optimization problem more complicated. A model-based method for optimizing the parameters of a PID controller with a frequency-domain criterion and closed-loop specifications is proposed in Harris and Mellichamp (1985).

The objective function is minimized with a version of the simplex method. Schei (1994) proposes a non-convex constrained optimization method to maximize the controller gain in low frequencies with constraints on the maximum of the sensitivity and complementary sensitivity functions. Åström et al. (1998) show that the maximum of the sensitivity function is an appropriate design variable and together with optimization of load disturbance rejection and

*Corresponding author. Tel.: +41 21 693 38 41; fax: +41 21 693 25 74.
E-mail address: alireza.karimi@epfl.ch (A. Karimi).

0967-0661/$ - see front matter © 2006 Elsevier Ltd. All rights reserved.
doi:10.1016/j.conengprac.2006.06.002

good choice of set point weight can give generally very high performances for PI controllers. An algorithm to find a local minimum of the criterion is proposed. Panagopoulos et al. (2002) extend this method to design PID controllers. A numerical solution to this non-convex problem is also developed in Hwang and Hsiao (2002).

Convex optimization approaches to fixed-order controller design are rather limited. In Grassi and Tsakalis (1996) a convex optimization method for PID controller tuning by open-loop shaping in frequency domain is proposed. The infinity-norm of the difference between the desired open-loop transfer function and the achieved one is minimized. This method, however, needs the desired open-loop transfer function to be defined and it cannot be applied to the case of multi-model uncertainty. Ho et al. (1997) show that all stabilizing PID controllers with fixed proportional gain can be found by resolving a linear programming problem for the derivative and integral gains. Blanchini et al. (2004) go further by showing that, given the value of the proportional gain, the region of the plane defined by the derivative and integral gains, where a considered H_∞ constraint is satisfied, consists of the union of disjoint convex sets. However, both methods have the drawback of fixing the proportional gain a priori. In Keel and Bhattacharyya (1997) a PID controller design based on linear programming for pole placement and model matching problem is proposed. A serious difficulty in this approach is to specify the desired closed-loop poles and desired closed-loop transfer function. Recently, a new approach based on the generalized Kalman–Yakoubovic–Popov lemma has been proposed to tune the linearly parameterized controllers in the Nyquist diagram (Hara et al., 2006). The idea is to define several convex regions in the complex plane and design the controller such that in each frequency interval the open-loop transfer function lies in one of the regions. However, this method seems to be too complex for industrial applications.

In this paper, a loop shaping method in the Nyquist diagram is proposed. A new stability margin is defined which guarantees a lower bound for the gain, phase and modulus margins (the inverse of the maximum of the sensitivity function). The main property of the new margin is that a constraint on this margin is linear with respect to the parameters of linearly parameterized controllers. Therefore, optimizing load disturbance rejection with constraint on this margin leads to a linear constrained optimization problem which can be solved by linear programming. A lower bound for the crossover frequency is also defined which also leads to a linear constraint for the optimization problem. With this constraint, an optimization problem to maximize the new robustness margin can be solved by linear programming. The method can be applied to stable plants represented by transfer functions with pure time delay or simply by non-parametric models in the frequency domain. The robustness of the closed-loop system with respect to unmodeled dynamics is ensured with the constraint on the new linear margin, while the multi-model uncertainty can be considered easily by increasing the number of constraints. The proposed method can be used for PID controllers as well as higher-order linearly parameterized controllers in discrete or continuous time. Standard linear optimization solvers can be used to find the global optimal controller. The proposed method is applied to a double-axis linear permanent magnet synchronous motor (LPMSM). This type of motors can be used for wafer fabrication and inspection and other high precision positioning systems. A generalized synchronization control for such systems has been proposed in Xiao et al. (2005).

This paper is organized as follows: in Section 2 the class of models, controllers and the control objectives are defined. Section 3 introduces a new linear stability margin, a lower bound on the crossover frequency and presents the linear optimization problem. Simulation results are given in Section 4 and experimental results in Section 5. Finally, Section 6 gives some concluding remarks.

2. Problem formulation

2.1. Plant model

The class of linear time-invariant SISO systems with no pole in the right half plane is considered. It is assumed that a set of non-parametric models in the frequency domain is available. This set can be obtained either by spectral analysis from several identification experiments at different operating points or from parametric models in the form of rational transfer functions with pure time delay. Suppose that the dynamics of the system can be captured by a sufficiently large finite number of frequency points N. The number of models in the set is m and so the model set can be presented by

$$\mathscr{M} \triangleq \{G_i(\mathrm{j}\omega_k) | i = 1, \ldots, m; \quad k = 1, \ldots, N\}. \tag{1}$$

2.2. Controller parameterization

The class of linearly parameterized controllers is considered:

$$K(s) = \rho^{\mathrm{T}} \phi(s), \tag{2}$$

where

$$\rho^{\mathrm{T}} = [\rho_1, \rho_2, \ldots, \rho_n], \tag{3}$$

$$\phi^{\mathrm{T}}(s) = [\phi_1(s), \phi_2(s), \ldots, \phi_n(s)], \tag{4}$$

n is the number of controller parameters and $\phi_i(s), i = 1, \ldots, n$, are transfer functions with no RHP pole. With this parameterization, every point on the Nyquist diagram of $K(\mathrm{j}\omega)G_i(\mathrm{j}\omega)$ can be written as a linear function of the controller parameters ρ:

$$\begin{aligned} K(\mathrm{j}\omega_k)G_i(\mathrm{j}\omega_k) &= \rho^{\mathrm{T}} \phi(\mathrm{j}\omega_k)G_i(\mathrm{j}\omega_k) \\ &= \rho^{\mathrm{T}} \mathscr{R}_i(\omega_k) + \mathrm{j}\rho^{\mathrm{T}} \mathscr{I}_i(\omega_k), \end{aligned} \tag{5}$$

where $\mathscr{R}_i(\omega_k)$ and $\mathscr{I}_i(\omega_k)$ are, respectively, the real and the imaginary parts of $\phi(j\omega_k)G_i(j\omega_k)$.

It should be mentioned that PID controllers are a special case of this parameterization with

$$\rho^{\mathrm{T}} = [K_p, K_i, K_d], \tag{6}$$

$$\phi^{\mathrm{T}}(s) = \left[1, \frac{1}{s}, \frac{s}{1+T_f s}\right], \tag{7}$$

where T_f (supposed to be known) is the time constant of the noise filter.

2.3. Design specifications

Optimizing load disturbance rejection is considered as the desired performance for the closed-loop system. In general, to reject low-frequency disturbances, the controller gain at low-frequencies should be maximized. For a rational continuous-time controller with fixed denominator $R(s)$,

$$K(s) = \frac{\rho_0 + \rho_1 s + \cdots + \rho_n s^n}{R(s)}, \tag{8}$$

it corresponds to maximizing ρ_0. For the particular case of the denominator containing only one integrator, maximizing ρ_0 corresponds to minimizing the integrated error (IE) defined by

$$\mathrm{IE} = \int_0^\infty e(t)\,\mathrm{d}t. \tag{9}$$

This can be proved by assuming that in (8) $R(s) = sR'(s)$ where

$$R'(s) = 1 + r_1 s + \cdots + r_{n-1} s^{n-1}. \tag{10}$$

Then, the control law becomes

$$u(t) + r_1 \frac{\mathrm{d}u}{\mathrm{d}t} + \cdots + r_{n-1} \frac{\mathrm{d}^{(n-1)}u}{\mathrm{d}t^{(n-1)}} = \rho_0 \int_0^\infty e(t)\,\mathrm{d}t + \rho_1 e(t) + \cdots + \rho_n \frac{\mathrm{d}^{(n-1)}e}{\mathrm{d}t^{(n-1)}}. \tag{11}$$

Furthermore, assume that the error is initially zero ($e(0) = 0$) and that a unit step disturbance is applied at the process input. Since the closed-loop system is stable and has integral action, the control error will go to zero at infinity ($e(\infty) = 0$). Thus,

$$u(\infty) - u(0) = \rho_0 \int_0^\infty e(t)\,\mathrm{d}t. \tag{12}$$

Since the disturbance is applied at the process input, the change in control signal is equal to the change of the disturbance:

$$u(\infty) - u(0) = 1. \tag{13}$$

Using (12) and (13), IE becomes

$$\mathrm{IE} = \frac{1}{\rho_0}. \tag{14}$$

Thus, if ρ_0 is maximized, the IE is minimized. For the special case of a PID controller, ρ_0 corresponds to K_i. Thus, maximizing K_i corresponds to minimizing IE.

Similarly, for a discrete-time rational controller with fixed denominator $R(z^{-1})$,

$$K(z^{-1}) = \frac{\rho_0 + \rho_1 z^{-1} + \cdots + \rho_n z^{-n}}{R(z^{-1})}, \tag{15}$$

the sum of the controller parameters $\sum_j \rho_j$ should be maximized for optimizing load disturbance rejection. For the particular case, when $R(z^{-1})$ contains only one integrator, maximizing the sum of controller parameters is equivalent to minimizing IE. It should be mentioned that IE is a good approximation of the integrated absolute error (IAE) for well-damped systems.

3. Controller design by linear programming

The classical robustness indicators like gain, phase and modulus margins as well as the performance indicator, the crossover frequency ω_c, are nonlinear functions of the controller parameters. The optimization methods with constraints on these values lead to non-convex optimization problems and cannot be solved efficiently. In this section a new stability margin together with a lower bound for the crossover frequency will be defined which leads to linear constraints for the optimization problems in which robustness and/or performance are maximized. These optimization problems can be solved efficiently by a linear programming approach.

For sake of simplicity, the linear constraints will be given for one model. In the multi-model case only the number of constraints will be increased by a factor m and the problems can still be solved by linear programming.

3.1. Linear robustness margin

Consider a straight line d_1 in the complex plane crossing the negative real axis between 0 and -1 with an angle $\alpha \in]0^\circ\ 90^\circ]$ (see Fig. 1). The new linear stability margin $\ell \in]0\ 1[$ is the distance between the critical point -1 and d_1 where it crosses the negative real axis. If the Nyquist curve of the open-loop transfer function lies on the right side of d_1, the following lower bounds on the conventional robustness margins are ensured (see Fig. 1):

$$G_m \geqslant \frac{1}{1-\ell}, \tag{16}$$

$$\Phi_m \geqslant \Phi_l = \arccos\left((1-\ell)\sin^2\alpha + \cos\alpha\sqrt{1-(1-\ell)^2\sin^2\alpha}\right), \tag{17}$$

$$M_m \geqslant M_l = \ell \sin\alpha, \tag{18}$$

where G_m, Φ_m and M_m are, respectively, the gain, phase and modulus margins and Φ_l and M_l, respectively, the

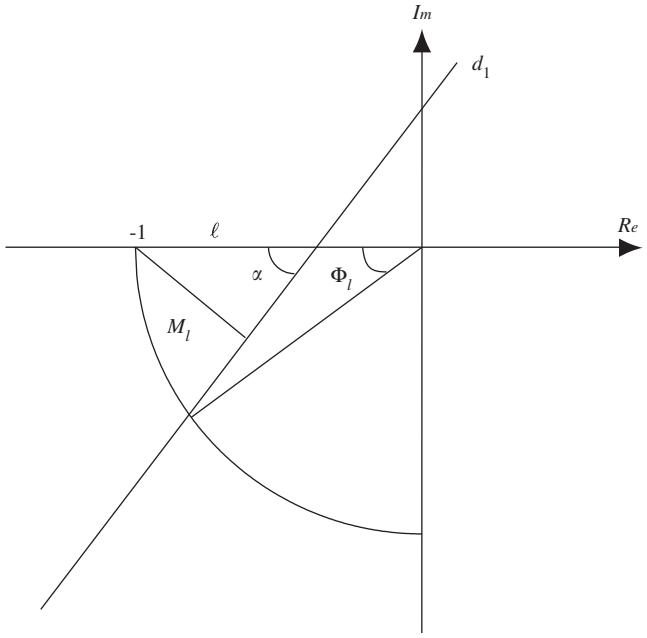

Fig. 1. New linear margin ℓ with respect to the classical robustness margins. The lower bounds for the phase and modulus margins are, respectively, Φ_l and M_l.

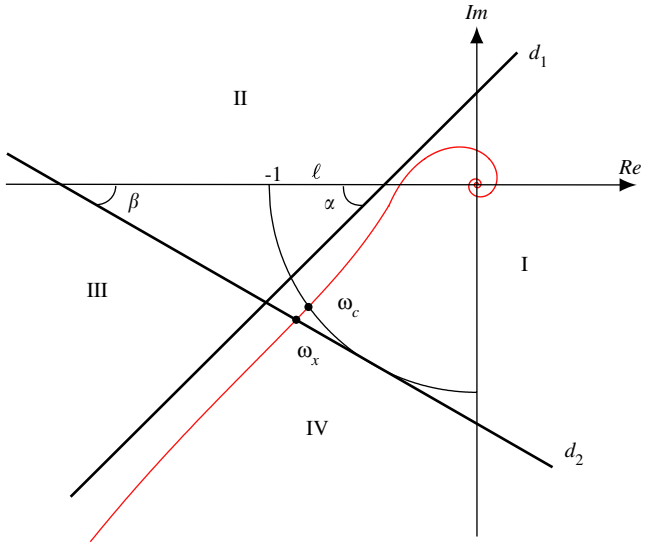

Fig. 2. Linear constraints for robustness and performance, with four regions: I, II, III and IV. The crossover frequency and the lower bound on the crossover frequency are, respectively, ω_c and ω_x.

lower bounds for the phase and modulus margins. For a fixed value of α, all lower bounds are increasing functions of the new margin ℓ. Therefore, ℓ can be used as a measure of robustness and can be maximized to optimize the robustness of the system. On the other hand, for a fixed value of ℓ, the phase and modulus margins increase with increasing α. As the modulus margin increases, the maximum of the sensitivity function decreases and consequently the system becomes better damped, but the bandwidth may decrease. This is due to the Bode sensitivity integral relation also called the area formula (Doyle et al., 1990). Thus, α can possibly be used as a design variable for tradeoff between the damping and the bandwidth of the closed-loop system. If two of the three conventional margins are given, it is easy to find the corresponding values for the linear margin. For example, if the gain margin must be 3 and the modulus margin 0.6, (16) imposes $\ell = 0.66$ and (18) imposes $\alpha = 64.16^\circ$. Generally, the typical values for the gain, phase and modulus margins are, respectively, between 2 and 5, 30° and 60° and 0.5 and 0.77 (Åström & Hägglund, 1995). Using (16), these values lead to a typical value between 0.5 and 0.8 for ℓ and using (17) and (18) to a typical value between 36.90° and 90° for α.

3.2. Lower bound on the crossover frequency

Consider another straight line d_2 in the complex plane tangent to the unit circle centered at the origin which crosses the negative real axis with angle β. The part of d_2 between d_1 and the imaginary axis is a linear approximation of the unit circle in this region. Now, assume that the open-loop Nyquist curve intersects d_2 at a frequency called ω_x. From Fig. 2 it is clear that the crossover frequency ω_c is always greater than or equal to ω_x. Hence, ω_x, which is a lower approximation for the crossover frequency, can be used as a measure of the time-domain performance (greater ω_x faster the disturbance rejection and smaller the rise time for tracking response). In order to prevent the Nyquist curve approaching the critical point from the left side at frequencies lower than ω_x, β should be chosen such that

$$\beta \leqslant \arcsin\left(\frac{1}{\ell+1}\right), \tag{19}$$

in order not to deteriorate the gain margin assured by d_1 and

$$\beta \leqslant \arcsin(1-\ell\sin\alpha), \tag{20}$$

in order not to deteriorate the modulus margin assured by d_1. For example, if ℓ is equal to 0.6 and α to 60°, β should be smaller than 28.71°.

3.3. Optimization for robustness

In this part, it is supposed that a desired crossover frequency ω_c is given and the objective is to find the best controller in terms of the robustness margins. The design variables for the optimization problem are ω_x, α and β. To guarantee an achieved crossover frequency greater than the desired one, ω_x is chosen equal to ω_c. As said in Section 3.1, α is chosen between 36.90° and 90° depending on the control objective. In order to have a good linear approximation of the unit circle $\beta = 30^\circ$ can be chosen (care should be taken to respect the inequalities (19) and (20)).

The design method is the same whether the open-loop transfer function $L(s)$ contains one or two integrators. The Nyquist diagram of $L(j\omega)$ at very low frequencies is located in region III or IV (depending on the number of integrators in $L(s)$) and at very high frequencies in region I (see Fig. 2). In order to ensure a certain distance from the critical point, the Nyquist curve should not enter region II. On the other hand, the Nyquist curve necessarily intersects d_2 at ω_x. As a result, the open-loop Nyquist curve $L(j\omega)$ should lie in region III or IV for frequencies less than ω_x and in region I for frequencies greater than ω_x. Thus, the following linear optimization problem is considered:

$$\begin{aligned} &\text{maximize} && \ell \\ &\text{subject to} && \rho^{\mathrm{T}}(\cot\alpha\,\mathscr{I}(\omega_k)-\mathscr{R}(\omega_k))+\ell\leqslant 1 && \text{for } \omega_k>\omega_x, \\ &&& \rho^{\mathrm{T}}(\cos\beta\,\mathscr{I}(\omega_k)+\sin\beta\,\mathscr{R}(\omega_k))>-1 && \text{for } \omega_k>\omega_x, \\ &&& \rho^{\mathrm{T}}(\cos\beta\,\mathscr{I}(\omega_k)+\sin\beta\,\mathscr{R}(\omega_k))\leqslant -1 && \text{for } \omega_k\leqslant\omega_x. \end{aligned} \tag{21}$$

The first line corresponds to the constraint that the Nyquist curve has to be below d_1 for $\omega_k>\omega_x$, the second line corresponds to the constraint that the Nyquist curve has to be above d_2 for $\omega_k>\omega_x$ and the third line corresponds to the constraint that the Nyquist curve has to be below d_2 for $\omega_k\leqslant\omega_x$. This optimization problem leads to the controller parameters that cancel the integral term if there is any in the controller (reducing the integral action increases the robustness of the closed-loop system). Therefore, in order to preserve the integral effect of the controller, for example, in a PID controller, a constraint $K_i>K_{\min}$ can be added to the constraints.

3.4. Optimization for performance

Another control objective is to consider some constraints for the robustness margins and optimize the closed-loop performance in terms of the load disturbance rejection. This can be done by maximizing ρ_0 (K_i for PID controllers) which also leads to minimizing the IE for the controller containing one integrator. The design variables are limited to the linear robustness margin ℓ and α. When $L(s)$ contains only one integrator, the open-loop Nyquist curve should lie in region I or IV, thus a simple optimization problem can be defined as follows:

$$\begin{aligned} &\text{maximize} && \rho_0 \\ &\text{subject to} && \rho^{\mathrm{T}}(\cot\alpha\,\mathscr{I}(\omega_k)-\mathscr{R}(\omega_k))+\ell\leqslant 1 && \text{for all } \omega_k. \end{aligned} \tag{22}$$

For the case of two integrators in $L(s)$, the constraints should be modified such that $L(j\omega)$ at low frequencies can be located in region III. This can be obtained using a straight line on the complex plane. The line d_2 can be used again to divide the complex plane in four regions. Once again β should be chosen in order to respect the inequalities (19) and (20). The optimization problem can be formulated as

$$\begin{aligned} &\text{maximize} && \rho_0 \\ &\text{subject to} && \rho^{\mathrm{T}}(\cot\alpha\,\mathscr{I}(\omega_k)-\mathscr{R}(\omega_k))+\ell\leqslant 1 && \text{for } \omega_k>\omega_x, \\ &&& \rho^{\mathrm{T}}(\cos\beta\,\mathscr{I}(\omega_k)+\sin\beta\,\mathscr{R}(\omega_k))\leqslant -1 && \text{for } \omega_k\leqslant\omega_x, \end{aligned} \tag{23}$$

where ω_x is this time not a lower approximation, but a lower bound for the crossover frequency as it can be located anywhere in region IV, and not necessarily at the intersection with d_1. A good choice for ω_x, in this case, is the open-loop bandwidth.

Remarks.

- The robustness and performance can be optimized simultaneously with a mixed criterion in the form of

$$\text{maximize} \quad \rho_0+\lambda\ell, \tag{24}$$

  where λ is a weighting factor to be chosen.
- The case of three integrators in $L(s)$ will be studied in the application example (see Section 5).
- The proposed approach to designing controllers does not take into consideration the input sensitivity function $U(s)$:

$$U(s)=\frac{K(s)}{1+K(s)G(s)}. \tag{25}$$

  Thus it is possible that the control input becomes too large when the closed-loop bandwidth is chosen much greater than the open-loop bandwidth. Two possibilities exist to resolve this problem:
  - Filter the reference signal with a first-order filter of the form $1/(1+Ts)$ to take out the high-frequency part of the signal.
  - Introduce additional constraints to prevent the input sensitivity function from being too large at high frequencies. Suppose that $K(s)G(s)$ is much smaller than 1 at high frequencies. Then, to limit $U(s)$ at high frequencies, additional constraints can be introduced to limit the magnitude of $K(s)$. To keep the method linear, the constraints are added on the real and imaginary parts of $K(s)$ instead of on its magnitude:

$$\begin{aligned} &-K_u<\rho^{\mathrm{T}}\mathscr{R}_\phi(\omega_k)<K_u \quad \text{for } \omega_k>\omega_u, \\ &-K_u<\rho^{\mathrm{T}}\mathscr{I}_\phi(\omega_k)<K_u \quad \text{for } \omega_k>\omega_u, \end{aligned} \tag{26}$$

    where $\mathscr{R}_\phi(\omega_k)$ and $\mathscr{I}_\phi(\omega_k)$ are, respectively, the real and the imaginary parts of $\phi(j\omega_k)$. K_u is the limit of the absolute value of the real and imaginary parts of $K(s)$ and ω_u is the frequency above which the constraints are applied.

4. Simulation results

The design method is tested on two different examples taken from Panagopoulos et al. (2002) to illustrate its properties.

4.1. Example 1

Consider the following parametric plant model:

$$G_1(s) = \frac{1}{(s+1)^3} e^{-5s}. \quad (27)$$

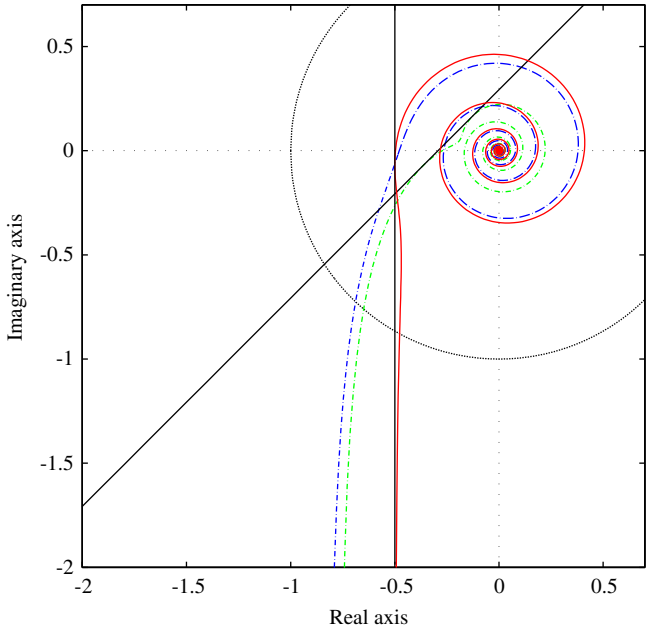

Fig. 3. Nyquist plots of the open-loop transfer functions for G_1 (solid: proposed method with $\ell = 0.5$ and $\alpha = 90^\circ$, dashed: proposed method with $\ell = 0.707$ and $\alpha = 45^\circ$, dashed-dotted: Panagopoulos' method).

This model captures typical dynamics with long dead time encountered in the process industry. Different PID controllers are designed and compared with those obtained with the method proposed by Panagopoulos et al. (2002). Panagopoulos' method is chosen to make the comparison, since it also designs PID controllers by optimizing the load disturbance rejection with constraints on the modulus margin. The particularity of Panagopoulos' method is that it uses a set point weight and also filters the reference signal with a first-order filter. To do a fair comparison between these two methods, the first-order filter used in Panagopoulos' method is also used in the proposed method.

It should be noted that Ziegler–Nichols' method gives very poor results for this example (Åström & Hägglund, 1995, pp. 145–146) so it is not considered in the comparison.

First of all the frequency response of G_1 is evaluated at $N = 8000$ equally spaced frequency points between 0 and 80 rad/s. Then PID controllers are designed for this plant using the optimization problem (22) to optimize the load disturbance rejection. The controller designed using Panagopoulos' method has a modulus margin equal to 0.5. A first controller is designed with ℓ fixed to 0.707 and α to 45° to obtain the same specification for the modulus margin. Then a second controller is designed with ℓ fixed to 0.5 and α to 90° to see the effect of α on the closed-loop responses. The time constant of the derivative part of the PID controllers T_f is set to 0.1 s.

The Nyquist plots of the open-loop transfer functions obtained with the proposed method and with Panagopoulos' method are shown in Fig. 3. It can be observed that the

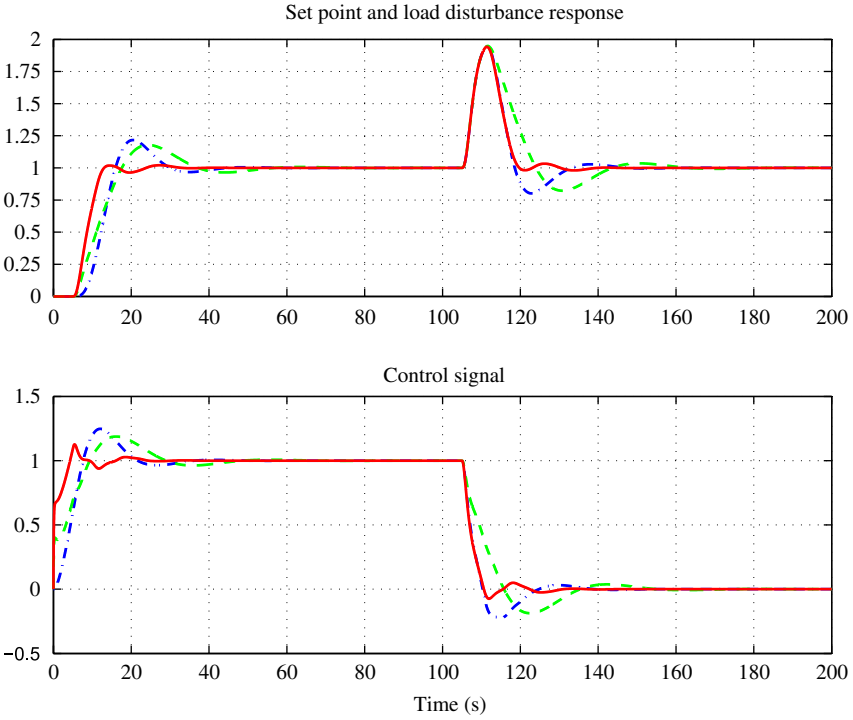

Fig. 4. Set point and load disturbance responses for G_1 (solid: proposed method with $\ell = 0.5$ and $\alpha = 90^\circ$, dashed: proposed method with $\ell = 0.707$ and $\alpha = 45^\circ$, dashed-dotted: Panagopoulos' method).

Nyquist plots obtained by the proposed method (solid and dashed) respect the constraint represented by the linear margin. The responses of the closed-loop systems to a set point change and load disturbance are compared in Fig. 4. It can be seen that for the proposed method with $\ell = 0.707$ and $\alpha = 45^\circ$, the overshoot of the load disturbance rejection is about the same as the one obtained with Panagopoulos' method, but the response is slower. The tracking response is significantly improved by the proposed method with $\ell = 0.5$ and $\alpha = 90^\circ$.

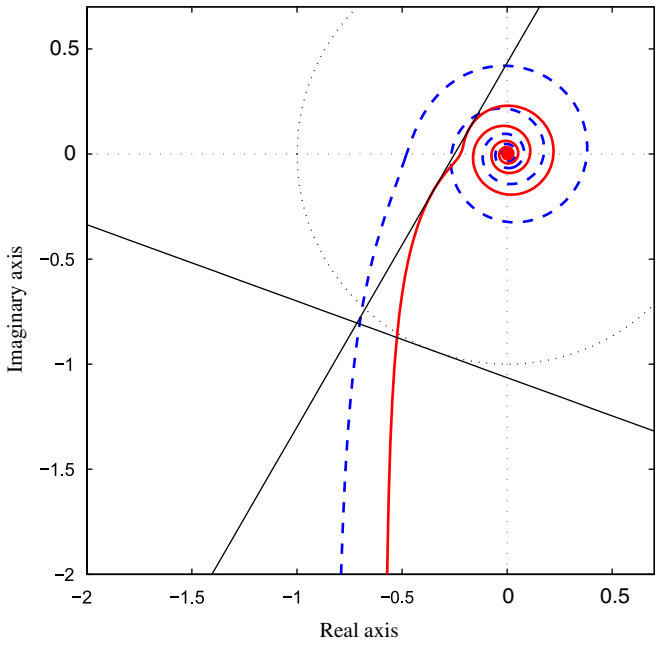

Fig. 5. Nyquist plots of the open-loop transfer functions for G_1 (solid: proposed method with the mixed criterion ($\alpha = 60^\circ$, $\beta = 20^\circ$, $\omega_x = 0.1$ rad/s, $\lambda = 50$), dashed: Panagopoulos' method).

Now, let the control objective be to maximize the robustness of the closed-loop system at the cost of reducing the crossover frequency from 0.17 to 0.1 rad/s. The constraints of (21) together with the mixed criterion (24) are used. In this approach, four parameters must be chosen. To have a crossover frequency of at least 0.1 rad/s, the lower approximation of the crossover frequency ω_x is set to 0.1 rad/s. To have a well-damped system, $\alpha = 60^\circ$ is chosen. To proceed one can start with $\beta = 20^\circ$ then according to the results this value can be slightly adapted to respect the inequalities (19) and (20). Finally, λ is tuned for the tradeoff between robustness and performance of the load disturbance rejection (for this example $\lambda = 50$ is chosen). The Nyquist plots of the open-loop transfer functions obtained with the proposed method using the mixed criterion and with Panagopoulos' method are shown in Fig. 5. It can be observed that the Nyquist plot obtained by the proposed method satisfies the constraints imposed by d_1 and d_2 and leads to a linear margin ℓ of 0.750 and a crossover frequency of 0.1 rad/s. The responses of the closed-loop systems to a set point change and load disturbance are compared in Fig. 6. Although the robustness is improved, the load disturbance rejection capability is still acceptable.

To facilitate the comparison between these controllers, the details of the designs, the related performances and robustness achieved are shown in Table 1, where ω_c stands

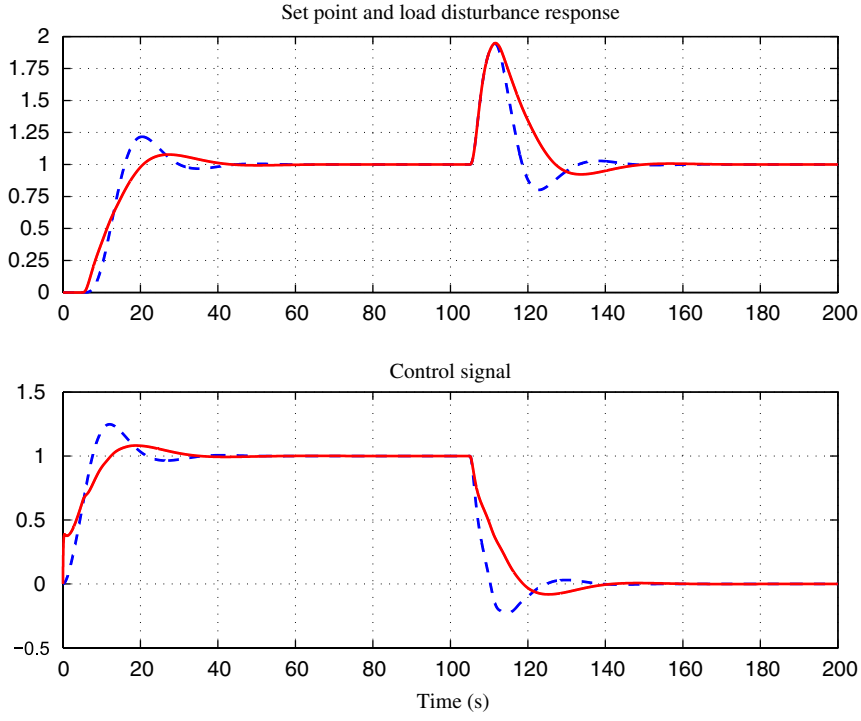

Fig. 6. Set point and load disturbance responses for G_1 (solid: proposed method with the mixed criterion ($\alpha = 60^\circ$, $\beta = 20^\circ$, $\omega_x = 0.1$ rad/s, $\lambda = 50$), dashed: Panagopoulos' method).

Table 1
Properties of the controllers obtained for the system G_1

Method	K_p	K_i	K_d	M_m	ω_c	o_s	t_s	IAE_s	o_d	t_d	IAE_d
Panagopoulo's method	0.555	0.173	0.966	0.50	0.17	21.68	41.70	14.21	94.50	44.31	9.10
max K_i ($\ell = 0.707, \alpha = 45^\circ$)	0.241	0.127	0.678	0.57	0.12	17.83	53.37	13.83	94.88	59.79	12.20
max K_i ($\ell = 0.5, \alpha = 90^\circ$)	0.608	0.139	1.039	0.50	0.14	2.04	30.57	9.16	94.27	37.02	7.54
max $K_i + 50\ell$ ($\alpha = 60^\circ$)	0.263	0.106	0.640	0.66	0.10	7.75	40.52	13.00	94.92	46.95	11.38

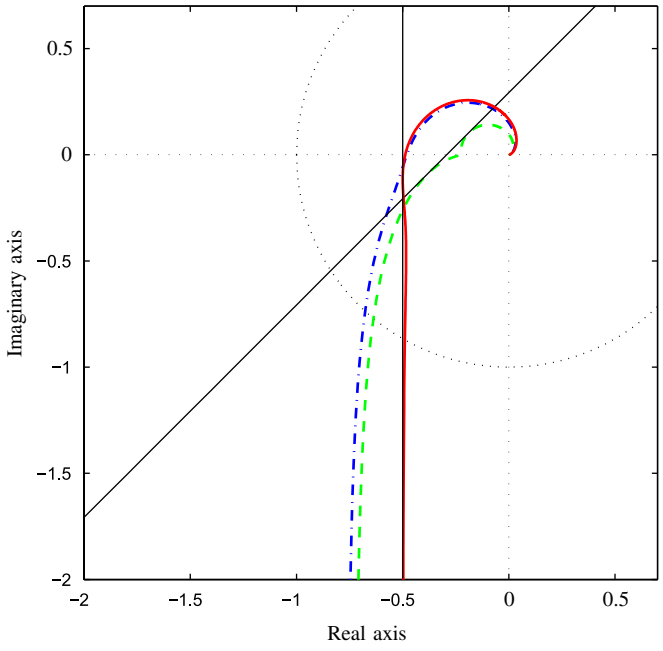

Fig. 7. Nyquist plots of the open-loop transfer functions for G_2 (solid: proposed method with $\ell = 0.5$ and $\alpha = 90^\circ$, dashed: proposed method with $\ell = 0.707$ and $\alpha = 45^\circ$, dashed-dotted: Panagopoulos' method).

for the crossover frequency (in rad/s), o_s for the overshoot (in %), t_s for the settling time to 1% (in s), IAE_s for the IAE of the set point change, o_d for the overshoot (in %), t_d for the settling time to 1% (in s) and IAE_d for the IAE of the load disturbance.

4.2. Example 2

Consider the following non-minimum phase model:

$$G_2(s) = \frac{1 - 2s}{(s+1)^3}. \tag{28}$$

Although a zero in the right half plane is uncommon in process control, this model is considered to demonstrate the wide applicability of the method.

The first step is to evaluate G_2 in $N = 8000$ equally spaced frequency points between 0 and 80 rad/s. Then two PID controllers for optimization of the load disturbance rejection are designed using the same specifications considered for G_1. The Nyquist plots of the open-loop transfer functions obtained with the proposed method and with Panagopoulos' method are shown in Fig. 7. It can be observed that the Nyquist plots obtained by the proposed method (solid and dashed) respect the constraint represented by the linear margin. The responses of the closed-loop systems to a set point change and load disturbance are compared in Fig. 8. It can be seen that for the proposed method with $\ell = 0.707$ and $\alpha = 45^\circ$ the overshoot of the load disturbance rejection is once again about the same as the one obtained with Panagopoulos' method, but the response is slower. The tracking response is significantly improved by the proposed method with $\ell = 0.5$ and $\alpha = 90^\circ$. To facilitate the comparison between the different controllers, the details of the designs are shown in Table 2.

In a general way, the proposed method gives about the same results as Panagopoulos' method in terms of load disturbance rejection. On the other hand, it gives better results in terms of set point tracking when the design parameters α is increased. Furthermore, this method is easier to implement, since it uses a linear programming approach compared to the non-convex optimization used by Panagopoulos' method.

5. Experimental results

The proposed method is applied to a LPMSM. The aim is to control the position of such a system, which is shown in Fig. 9. LPMSMs have high acceleration and deceleration capabilities, high mechanical stiffness, reduced friction and no mechanical transmission. They, therefore, do not suffer from backlash and thus allow very high positioning accuracy to be achieved. In this application, the dynamics of each axis depend on the position of the two axes. For example, it is clear that the dynamics of the lower axis change in function of the position of the moving part of the higher axis. If the moving part of the higher axis is at an extremity, it is connected to the lower axis with a different rigidity from the case that the moving part is at the center. This property was highlighted by system identification in different positions. The stroke of each axis (32 cm) is divided into eight equally spaced partitions which gives a grid of 81 nodes. The system is excited with a sum of sinusoidal signals from 8.8 to 3000 Hz at each position and thus 81 non-parametric models in the frequency domain are obtained. Fig. 10 shows the magnitude Bode diagram of the identified models for the higher axis (see Fig. 9). There

Table 2
Properties of the controllers obtained for the system G_2

Method	K_p	K_i	K_d	M_m	ω_c	o_s	t_s	IAE$_s$	o_d	t_d	IAE$_d$
Panagopoulo's method	0.542	0.262	0.428	0.50	0.28	10.19	17.71	7.92	107.34	18.94	6.11
max K_i ($\ell = 0.707, \alpha = 45^\circ$)	0.247	0.196	0.278	0.56	0.19	14.08	30.45	8.09	97.74	34.18	8.23
max K_i ($\ell = 0.5, \alpha = 90^\circ$)	0.541	0.208	0.428	0.51	0.23	0.15	12.69	5.85	103.02	16.67	6.10

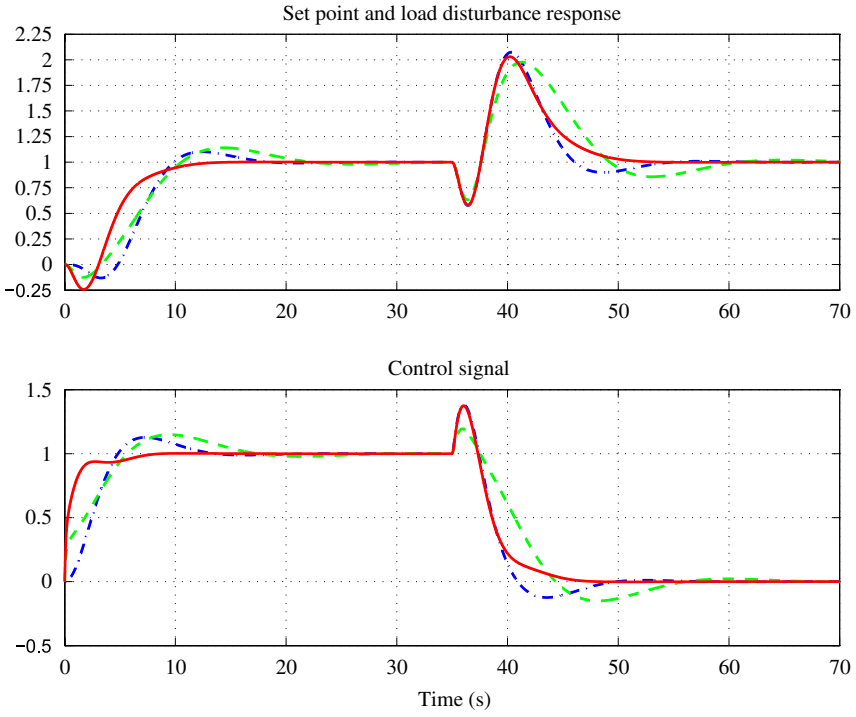

Fig. 8. Set point and load disturbance responses for G_2 (solid: proposed method with $\ell = 0.5$ and $\alpha = 90^\circ$, dashed: proposed method with $\ell = 0.707$ and $\alpha = 45^\circ$, dashed-dotted: Panagopoulos' method).

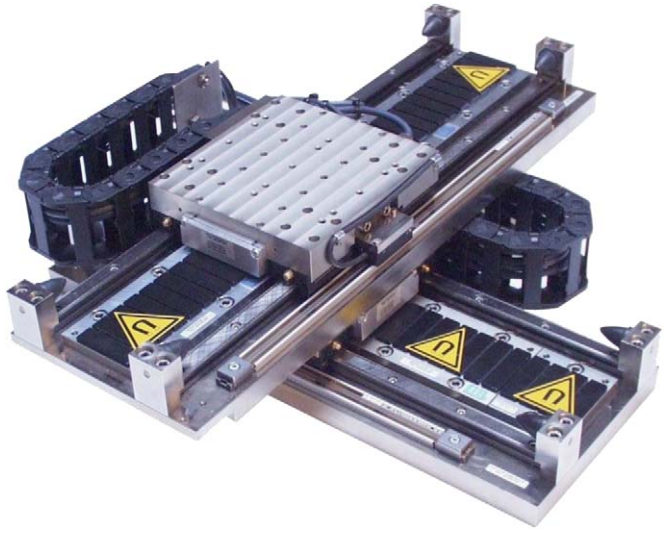

Fig. 9. Double-axis linear permanent magnet synchronous motor (with courtesy of ETEL).

is a large model variation at low frequencies (from 10 to 30 Hz) due to the effect of the axes positions and at high frequencies due to the measurement noise.

For the axis, whose dynamics are shown in Fig. 10, a low-order controller should be designed with a closed-loop bandwidth of at least 140 Hz (specified by the industrial partner) and robust with respect to the friction parameter variations. This problem matches perfectly with the problem formulation of the proposed method. The robustness with respect to the axes positions is considered by a model set containing the 81 identified models, while the robustness with respect to the friction parameter variations and high-frequency uncertainties are taken into account by a linear margin $\ell = 0.7$ and $\alpha = 45^\circ$.

The motor position is measured by an analog position encoder having a resolution of 0.24 nm. Each motor used in the experiment is controlled by a two-degree of freedom polynomial controller operating at a sampling frequency of 18 kHz.

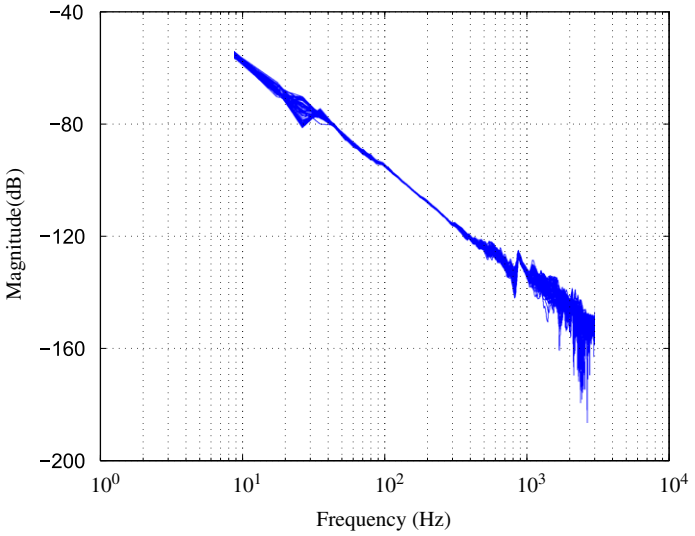

Fig. 10. The magnitude Bode diagram of 81 identified models for the higher axis.

The aim of the design is to optimize the load disturbance rejection at the plant input. Therefore, the controller should contain an integrator and IE should be minimized. Let the following structure be considered for the feedback part of the controller:

$$K(z^{-1}) = \frac{S(z^{-1})}{R(z^{-1})}, \tag{29}$$

where

$$S(z^{-1}) = \rho_1 + \rho_2 z^{-1} + \cdots + \rho_n z^{-n+1} \tag{30}$$

and the polynomial $R(z^{-1})$ is fixed to

$$R(z^{-1}) = (1 - z^{-1}). \tag{31}$$

The slope of the Bode diagram at low frequencies shows the existence of two integrators in the plant model which leads to an open-loop transfer function with three integrators. Consequently, at very low frequencies the Nyquist diagram will be located in region II (see Fig. 2) but very far from the critical point. Suppose that the Nyquist diagram intersects d_2 in ω_l. Then, at middle frequencies (frequencies between ω_l and ω_x), the Nyquist diagram is below d_2 (in regions III and IV) and at high frequencies in region I. For discrete-time controllers, the control objective is equivalent to maximizing the sum of the parameters of the polynomial $S(z^{-1})$. Hence, the following optimization problem is considered:

$$\begin{aligned}
&\text{maximize} \quad \sum_{j=1}^{n} \rho_j \\
&\text{subject to} \quad \rho^{\mathrm{T}}(\cot\alpha\, \mathscr{I}_i(\omega_k) - \mathscr{R}_i(\omega_k)) + \ell \leqslant 1 \qquad \text{for } \omega_k > \omega_x, \\
&\qquad i = 1, \ldots, 81, \\
&\qquad \rho^{\mathrm{T}}(\cos\beta\, \mathscr{I}_i(\omega_k) + \sin\beta\, \mathscr{R}_i(\omega_k)) \leqslant -1 \qquad \text{for } \omega_l < \omega_k \leqslant \omega_x, \\
&\qquad i = 1, \ldots, 81,
\end{aligned} \tag{32}$$

where

$$\mathscr{R}_i(\omega_k) = \mathrm{Re}[\phi(\mathrm{e}^{-\mathrm{j}\omega_k h}) G_i(\mathrm{e}^{-\mathrm{j}\omega_k h})], \tag{33}$$

$$\mathscr{I}_i(\omega_k) = \mathrm{Im}[\phi(\mathrm{e}^{-\mathrm{j}\omega_k h}) G_i(\mathrm{e}^{-\mathrm{j}\omega_k h})], \tag{34}$$

$$\phi^{\mathrm{T}}(\mathrm{e}^{-\mathrm{j}\omega_k h}) = \frac{1}{1 - \mathrm{e}^{-\mathrm{j}\omega_k h}} [1, \mathrm{e}^{-\mathrm{j}\omega_k h}, \ldots, \mathrm{e}^{-\mathrm{j}(n-1)\omega_k h}] \tag{35}$$

and h is the sampling period.

First, a second-order controller (equivalent to a discrete-time PID controller) is designed. As mentioned before, the linear robustness margin ℓ is set to 0.7 and α to 45°. The lower bound of the crossover frequency ω_x is set to 140 Hz and ω_l to 80 Hz. Finally, β is set to 30° in order to respect the inequalities (19) and (20). The Nyquist plots of the open-loop transfer function for the 81 models obtained with this method are shown in Fig. 11. It can be noticed that the constraints are respected, thus a minimal robustness margin and a minimal bandwidth are assured for all the models. The load disturbance response of the second-order controller (dashed-dotted line) at the middle of the grid is shown in Fig. 12. The load disturbance response is generated by adding a step disturbance at the input of the system, simulating an external force disturbance of 5.87 N. This disturbance is not really realistic, but it is the only way to test the designed controller. The set point response is not included, since a two-degree of freedom controller is used for this application. Thus the feedforward part still needs to be designed.

In order to improve the result in terms of load disturbance rejection, a higher-order controller (fourth order) is designed. The same specifications as for the second-order controller are used. The result is shown in Fig. 12 (dashed line). The load disturbance rejection is

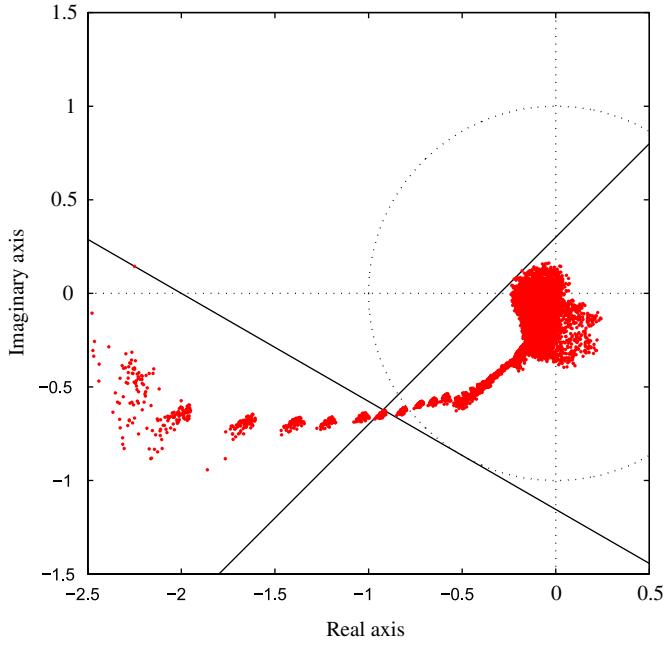

Fig. 11. Nyquist plots of the open-loop transfer function for the 81 models obtained with the second-order controller ($\max \sum_j \rho_j$).

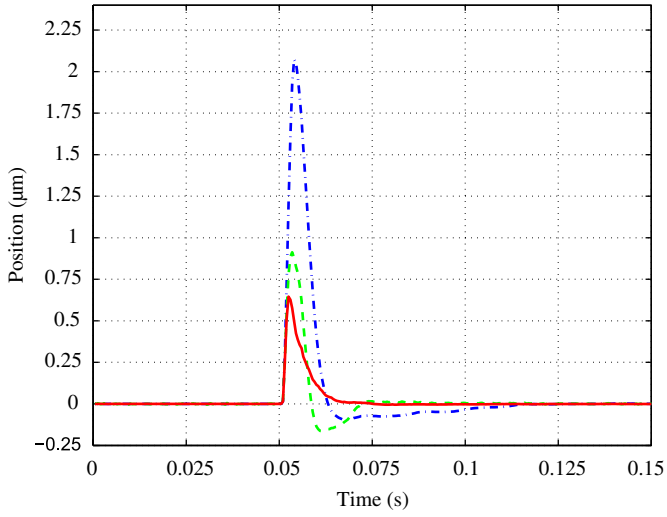

Fig. 12. Load disturbance responses: second-order controller ($\max \sum_j \rho_j$) (dashed-dotted), fourth-order controller ($\max \sum_j \rho_j$) (dashed), fifth-order controller ($\max \ell$ with $\sum_j \rho_j > K_{\min}$) (solid).

really improved, since the overshoot due to the disturbance is divided by more than 2.

Now, suppose that the load disturbance rejection and the crossover frequency of the fourth-order controller are satisfactory, but that it is required to increase the linear robustness margin. To fulfill this requirement, a higher-order controller (fifth order) is designed using the optimization problem (21) with some small modifications. In this optimization problem, the limit represented by ω_x between the low and high frequencies is really hard to respect. Frequencies over ω_x have to be in region I, whereas frequencies under ω_x have to be in region III or IV (see Fig. 2). Since in this application 81 models are used, the limit between low and high frequencies cannot be respected for all the models, thus it can be softened by adding a margin for ω_x. Frequencies over $\omega_x + m$ have to be in region I, whereas frequencies under $\omega_x - m$ have to be in region III or IV. Due to the open-loop transfer function that contains three integrators, the Nyquist diagram at very low frequencies will be located in region II (see Fig. 2). Finally, an additional constraint on the sum of the parameters is also added in order to preserve the performance in terms of the load disturbance rejection achieved with the fourth-order controller. Hence, the following optimization problem is considered:

$$
\begin{aligned}
&\text{maximize} \quad \ell \\
&\text{subject to} \quad \rho^{\mathrm{T}}(\cot\alpha\, \mathscr{I}_i(\omega_k) - \mathscr{R}_i(\omega_k)) + \ell \leqslant 1 \\
&\qquad \text{for } \omega_k > \omega_x + m, \;\; i = 1, \ldots, 81, \\
&\qquad \rho^{\mathrm{T}}(\cos\beta\, \mathscr{I}_i(\omega_k) + \sin\beta\, \mathscr{R}_i(\omega_k)) > -1 \\
&\qquad \text{for } \omega_k > \omega_x + m, \;\; i = 1, \ldots, 81, \\
&\qquad \rho^{\mathrm{T}}(\cos\beta\, \mathscr{I}_i(\omega_k) + \sin\beta\, \mathscr{R}_i(\omega_k)) \leqslant -1 \\
&\qquad \text{for } \omega_l < \omega_k \leqslant \omega_x - m, \;\; i = 1, \ldots, 81, \\
&\qquad \sum_{j=1}^{n} \rho_j \geqslant K_{\min}. \qquad (36)
\end{aligned}
$$

As the crossover frequency obtained with the fourth-order controller is equal to 269.69 Hz, the lower approximation of the crossover frequency ω_x is set to 268 Hz. Then ω_l is set to 80 Hz, α to 45° and β to 25° (in order to satisfy the inequalities (19) and (20) for a greater value of ℓ). Finally, $K_{\min}$ is equal to the sum of the parameters achieved by the fourth-order controller. The load disturbance rejection of the designed controller is shown in Fig. 12 (solid line). To facilitate the comparison, the details of the designs are shown in Table 3, where ω_c stands for the crossover frequency (in Hz), $M_{m,\min}$ for the minimum modulus margin of the 81 models, o_d for the overshoot of the load disturbance response (in μm) and t_d for the settling time to 1% of the biggest overshoot (in s). Although the fourth- and fifth-order controllers have the same sum of parameters, the fifth-order controller has a better load disturbance rejection capability (smaller overshoot, settling time and IAE). This is explained by the fact that maximizing the sum of the parameters minimizes IE (which is about the same for the two controllers) and not IAE. The fifth-order controller has been designed to increase the linear robustness margin ℓ which is the case, but it should be noted that it does not lead automatically to a bigger modulus margin.

In this application, the 81 identified models seem to be close to each other. By reducing the number of models and also the number of frequency points, similar results would be obtained for the controllers. However, the 81 identified

Table 3
Properties of the controllers obtained for the application

Method	ω_c	$M_{m,\min}$	ℓ	$\sum_j \rho_j$	o_d	t_d	IAE_d	IE_d
$\max \sum_j \rho_j$ (order 2)	150.54	0.632	0.70	1566	2.07	0.056	0.0146	0.0093
$\max \sum_j \rho_j$ (order 4)	269.69	0.652	0.70	4856	0.91	0.020	0.0061	0.0031
$\max \ell$ with $\sum_j \rho_j > K_{\min}$ (order 5)	293.69	0.584	0.73	4856	0.65	0.014	0.0036	0.0033

models and the high number of frequency points are kept to compute the controllers, in order to illustrate the capability of the linear programming approach to deal with a large number of constraints. Thus, no effort is done to reduce the number of models and frequency points.

6. Conclusions

Robust fixed-order controller design is formulated as a linear optimization problem. The proposed method is based on frequency loop shaping in the Nyquist diagram. The classical robustness and performance specifications are represented as linear constraints in the Nyquist diagram. There are only a few design variables which are directly related to the robustness (linear margin ℓ and α) and performance (lower approximation of the crossover frequency ω_x) of the closed-loop system. The control objective is to maximize the robustness margin or optimize the closed-loop performance in terms of the load disturbance rejection. The method is very simple and requires only the frequency response of the plant. Multi-model uncertainty can be taken into account straightforwardly. The method is very appropriate for PID controller design, yet it can be applied to higher-order linearly parameterized controllers in discrete or continuous time.

Simulation results showed that the method can be applied to the systems with large time delay as well as non-minimum phase systems. In comparison with the recently robust PID controller approaches, the proposed method is easy to understand and implement using the standard optimization tools.

The application of the proposed method on a double-axis positioning system has illustrated the capability of the approach to robust control of systems with large parameter variations with a restricted-order controller.

Acknowledgments

The authors acknowledge the collaborations of Ralph Coleman, Michel Mathia and Vincent Very from the company ETEL for real-time experiments.

References

Åström, K. J., & Hägglund, T. (1995). *PID controllers: Theory, design, and tuning* (2nd ed.). Instrument Society of America.

Åström, K. J., Panagopoulos, H., & Hägglund, T. (1998). Design of PI controllers based on non-convex optimization. *Automatica*, *34*(5), 585–601.

Blanchini, F., Lepschy, A., Miani, S., & Viaro, U. (2004). Characterization of PID and lead/lag compensators satisfying given $\mathscr{H}_\infty$ specifications. *IEEE Transactions on Automatic Control*, *49*(5), 736–740.

Doyle, J. C., Francis, B. A., & Tannenbaum, A. R. (1990). *Feedback control theory*. New York: Macmillan Publishing Co.

Grassi, E., & Tsakalis, K. (1996). PID controller tuning by frequency loop-shaping. In *Proceedings of the 35th conference on decision and control* (pp. 4776–4781). Kobe, Japan.

Grigoriadis, K. M., & Skelton, R. E. (1996). Low-order control design for LMI problems using alternating projection methods. *Automatica*, *32*(8), 1117–1125.

Hara, S., Iwasaki, T., & Shiokata, D. (2006). Robust PID control using generalized KYP synthesis: Direct open-loop shaping in multiple frequency ranges. *IEEE Control Systems Magazine*, *26*(1), 80–91.

Harris, S. L., & Mellichamp, D. A. (1985). Controller tuning using optimization to meet multiple closed-loop criteria. *AIChE Journal*, *31*(3), 484–487.

Ho, M.-T., Datta, A., & Bhattacharyya, S. (1997). A linear programming characterization of all stabilizing PID controllers. In *Proceedings of the American control conference* (pp. 3922–3928). Albuquerque, NM, USA.

Hwang, C., & Hsiao, C. Y. (2002). Solution of a non-convex optimization arising in PI/PID control design. *Automatica*, *38*(11), 1895–1904.

Keel, L. H., & Bhattacharyya, S. P. (1997). A linear programming approach to controller design. In *36th conference on decision and control* (pp. 2139–2148). San Diego, CA, USA.

Malan, S. A., Milanese, M., & Taragna, M. (1994). Robust tuning for PID controllers with multiple performance specifications. In *Proceedings of the 33rd conference on decision and control* (pp. 2684–2689). Lake Buena Vista, FL, USA.

Panagopoulos, H., Åström, K. J., & Hägglund, T. (2002). Design of PID controllers based on constrained optimisation. *IEE Proceedings Control Theory and Applications*, *149*(1), 32–40.

Schei, T. S. (1994). Automatic tuning of PID controllers based on transfer function estimation. *Automatica*, *30*(12), 1983–1989.

Xiao, Y., Zhu, K., & Liaw, H. C. (2005). Generalized synchronization control of multi-axis motion systems. *Control Engineering Practice*, *13*(7), 809–819.